PHYSICAL REVIEW D **79,** 071101(R) (2009)

Measurement of the $e^+e^- \to J/\psi c\bar{c}$ cross section at $\sqrt{s} \approx 10.6$ GeV

P. Pakhlov,[14] H. Aihara,[44] K. Arinstein,[1,32] T. Aushev,[19,14] A. M. Bakich,[39] V. Balagura,[14] E. Barberio,[22] A. Bay,[19] K. Belous,[13] V. Bhardwaj,[34] A. Bondar,[1,32] M. Bračko,[21,15] J. Brodzicka,[9] T. E. Browder,[8] M.-C. Chang,[5] P. Chang,[27] A. Chen,[25] B. G. Cheon,[7] R. Chistov,[14] S.-K. Choi,[50] Y. Choi,[38] M. Danilov,[14] M. Dash,[48] A. Drutskoy,[3] W. Dungel,[12] S. Eidelman,[1,32] D. Epifanov,[1,32] N. Gabyshev,[1,32] P. Goldenzweig,[3] B. Golob,[20,15] H. Ha,[17] B.-Y. Han,[17] K. Hayasaka,[23] H. Hayashii,[24] M. Hazumi,[9] Y. Horii,[43] Y. Hoshi,[42] W.-S. Hou,[27] Y. B. Hsiung,[27] H. J. Hyun,[18] T. Iijima,[23] K. Inami,[23] A. Ishikawa,[35] H. Ishino,[45,*] Y. Iwasaki,[9] N. J. Joshi,[40] D. H. Kah,[18] H. Kaji,[23] H. Kawai,[2] T. Kawasai,[30] H. Kichimi,[9] H. O. Kim,[18] Y. I. Kim,[18] K. Kinoshita,[3] B. R. Ko,[17] S. Korpar,[21,15] P. Križan,[20,15] P. Krokovny,[9] A. Kuzmin,[1,32] Y.-J. Kwon,[49] S.-H. Kyeong,[49] J. S. Lange,[6] M. J. Lee,[37] S. E. Lee,[37] T. Lesiak,[28,4] S.-W. Lin,[27] Y. Liu,[23] D. Liventsev,[14] R. Louvot,[19] F. Mandl,[12] A. Matyja,[28] S. McOnie,[39] H. Miyata,[30] Y. Miyazaki,[23] R. Mizuk,[14] Y. Nagasaka,[10] M. Nakao,[9] H. Nakazawa,[25] K. Nishimura,[8] O. Nitoh,[47] S. Ogawa,[41] T. Ohshima,[23] S. Okuno,[16] H. Ozaki,[9] G. Pakhlova,[14] H. Palka,[28] C. W. Park,[38] H. Park,[18] H. K. Park,[18] K. S. Park,[38] R. Pestotnik,[15] L. E. Piilonen,[48] A. Poluektov,[1,32] H. Sahoo,[8] Y. Sakai,[9] O. Schneider,[19] C. Schwanda,[12] K. Senyo,[23] M. E. Sevior,[22] M. Shapkin,[13] C. P. Shen,[8] J.-G. Shiu,[27] B. Shwartz,[1,32] J. B. Singh,[34] A. Sokolov,[13] S. Stanič,[31] M. Starič,[15] T. Sumiyoshi,[46] M. Tanaka,[9] G. N. Taylor,[22] Y. Teramoto,[33] I. Tikhomirov,[14] K. Trabelsi,[9] T. Tsuboyama,[9] S. Uehara,[9] T. Uglov,[14] Y. Unno,[7] S. Uno,[9] Y. Usov,[1,32] G. Varner,[8] K. Vervink,[19] A. Vinokurova,[1,32] C. H. Wang,[26] P. Wang,[11] Y. Watanabe,[16] R. Wedd,[22] E. Won,[17] B. D. Yabsley,[39] Y. Yamashita,[29] C. C. Zhang,[11] Z. P. Zhang,[36] V. Zhilich,[1,32] V. Zhulanov,[1,32] T. Zivko,[15] A. Zupanc,[15] and O. Zyukova[1,32]

(The Belle Collaboration)

[1]*Budker Institute of Nuclear Physics, Novosibirsk, Russia*
[2]*Chiba University, Chiba, Japan*
[3]*University of Cincinnati, Cincinnati, Ohio 45221, USA*
[4]*T. Kościuszko Cracow University of Technology, Krakow, Poland*
[5]*Department of Physics, Fu Jen Catholic University, Taipei, Taiwan*
[6]*Justus-Liebig-Universität Gießen, Gießen, Germany*
[7]*Hanyang University, Seoul, Korea*
[8]*University of Hawaii, Honolulu, Hawaii 96822, USA*
[9]*High Energy Accelerator Research Organization (KEK), Tsukuba, Japan*
[10]*Hiroshima Institute of Technology, Hiroshima, Japan*
[11]*Institute of High Energy Physics, Chinese Academy of Sciences, Beijing, China*
[12]*Institute of High Energy Physics, Vienna, Austria*
[13]*Institute of High Energy Physics, Protvino, Russia*
[14]*Institute for Theoretical and Experimental Physics, Moscow, Russia*
[15]*J. Stefan Institute, Ljubljana, Slovenia*
[16]*Kanagawa University, Yokohama, Japan*
[17]*Korea University, Seoul, Korea*
[18]*Kyungpook National University, Taegu, Korea*
[19]*École Polytechnique Fédérale de Lausanne (EPFL), Lausanne, Switzerland*
[20]*Faculty of Mathematics and Physics, University of Ljubljana, Ljubljana, Slovenia*
[21]*University of Maribor, Maribor, Slovenia*
[22]*University of Melbourne, School of Physics, Victoria 3010, Australia*
[23]*Nagoya University, Nagoya, Japan*
[24]*Nara Women's University, Nara, Japan*
[25]*National Central University, Chung-li, Taiwan*
[26]*National United University, Miao Li, Taiwan*
[27]*Department of Physics, National Taiwan University, Taipei, Taiwan*
[28]*H. Niewodniczanski Institute of Nuclear Physics, Krakow, Poland*
[29]*Nippon Dental University, Niigata, Japan*
[30]*Niigata University, Niigata, Japan*
[31]*University of Nova Gorica, Nova Gorica, Slovenia*
[32]*Novosibirsk State University, Novosibirsk, Russia*
[33]*Osaka City University, Osaka, Japan*
[34]*Panjab University, Chandigarh, India*
[35]*Saga University, Saga, Japan*
[36]*University of Science and Technology of China, Hefei, China*

[37]Seoul National University, Seoul, Korea
[38]Sungkyunkwan University, Suwon, Korea
[39]University of Sydney, Sydney, New South Wales, Australia
[40]Tata Institute of Fundamental Research, Mumbai, India
[41]Toho University, Funabashi, Japan
[42]Tohoku Gakuin University, Tagajo, Japan
[43]Tohoku University, Sendai, Japan
[44]Department of Physics, University of Tokyo, Tokyo, Japan
[45]Tokyo Institute of Technology, Tokyo, Japan
[46]Tokyo Metropolitan University, Tokyo, Japan
[47]Tokyo University of Agriculture and Technology, Tokyo, Japan
[48]IPNAS, Virginia Polytechnic Institute and State University, Blacksburg, Virginia 24061, USA
[49]Yonsei University, Seoul, Korea
[50]Gyeongsang National University, Chinju, Korea
(Received 19 January 2009; published 16 April 2009)

We present a new measurement of the $e^+e^- \to J/\psi c\bar{c}$ cross section where the $c\bar{c}$ pair can fragment either into charmed hadrons or a charmonium state. In the former case the J/ψ and a charmed hadron are reconstructed, while the latter process is measured using the recoil mass technique, which allows the identification of two-body final states without reconstruction of one of the charmonia. The measured $e^+e^- \to J/\psi c\bar{c}$ cross section is $(0.74 \pm 0.08\,^{+0.09}_{-0.08})$ pb, and the $e^+e^- \to J/\psi X_{\text{non-}c\bar{c}}$ cross section is $(0.43 \pm 0.09 \pm 0.09)$ pb. We note that the measured cross sections are obtained from a data sample with the multiplicity of charged tracks in the event larger than 4; corrections for the effect of this requirement are not performed as this cannot be done in a model-independent way. The analysis is based on a data sample with an integrated luminosity of 673 fb^{-1} recorded near the $\Upsilon(4S)$ resonance with the Belle detector at the KEKB e^+e^- asymmetric-energy collider.

DOI: 10.1103/PhysRevD.79.071101 PACS numbers: 13.66.Bc, 12.38.Bx, 14.40.Gx

Prompt charmonium production in e^+e^- annihilation is important for studying the interplay between perturbative QCD and nonperturbative effects. The J/ψ production rate and kinematic characteristics are poorly described by theory, and even the production mechanisms are not understood. An effective field theory, nonrelativistic QCD (NRQCD), predicts that prompt J/ψ production at $\sqrt{s} \approx 10.6$ GeV is dominated by $e^+e^- \to J/\psi gg$ with a 1 pb cross section [1]; the $e^+e^- \to J/\psi g$ contribution, which may be of the same order, is uncertain due to poorly constrained color-octet matrix elements [2]. The $e^+e^- \to J/\psi c\bar{c}$ cross section is predicted to be $\sim$0.1 pb [3], only $\sim$10% of that for $J/\psi gg$ [4]. By contrast, Belle observed the ratio of the $J/\psi c\bar{c}$ and inclusive J/ψ production cross sections to be $0.59^{+0.15}_{-0.13} \pm 0.12$ [5], and thus found $\sigma(e^+e^- \to J/\psi c\bar{c})/\sigma(e^+e^- \to J/\psi gg) \gtrsim 1$. Some authors have been able to reproduce this result using next-to-leading (NLO) corrections [6], or within the Regge trajectory approach [7].

In this report we present a new measurement of the $e^+e^- \to J/\psi c\bar{c}$ cross section. This process can be experimentally tagged by the presence of another charmed particle (either charmonium or charmed hadrons) in the event in addition to the reconstructed J/ψ. The technique used in this analysis allows the model dependence of the result to be removed, reducing the systematic uncertainties. Production of the J/ψ via mechanisms other than $e^+e^- \to J/\psi c\bar{c}$ is also studied. The analysis is performed using data recorded at the $\Upsilon(4S)$ and in the continuum 60 MeV below the resonance, corresponding to integrated luminosities of 605 fb^{-1} and 68 fb^{-1}, respectively. The data are collected with the Belle detector [8] at the KEKB asymmetric-energy e^+e^- collider [9].

We use a selection procedure similar to that described in Ref. [5]. All charged tracks are required to be consistent with originating from the interaction point (IP). Charged kaon and proton candidates are required to be positively identified. No identification requirements are applied for pion candidates. $K_S^0(\Lambda^0)$ candidates are reconstructed by combining $\pi^+\pi^-$ $(p\pi^-)$ pairs with an invariant mass within 10 MeV$/c^2$ of the nominal $K_S^0(\Lambda^0)$ mass. We require the distance between the tracks at the $K_S^0(\Lambda^0)$ vertex to be less than 1 cm, the transverse flight distance from the IP to be greater than 1 mm, and the angle between the $K_S^0(\Lambda^0)$ momentum direction and its decay path to be smaller than 0.1 rad. Photons are reconstructed in the electromagnetic calorimeter as showers with energies more than 50 MeV that are not associated with charged tracks.

J/ψ candidates are reconstructed via the $J/\psi \to \ell^+\ell^-$ $(\ell = e, \mu)$ decay channel. Two positively identified lepton candidates are required to form a common vertex that is less than 1 mm from the IP in the plane perpendicular to the beam axis ($\approx 98\%$ efficiency). A partial correction for final state radiation and bremsstrahlung energy loss is

*Now at Okayama University, Okayama, Japan.

performed by including the four-momentum of every photon detected within a 50 mrad cone around the $e^{\pm}$ direction in the e^+e^- invariant mass calculation. The J/ψ signal region is defined by $|M_{\ell^+\ell^-} - m_{J/\psi}| < 30\ \mathrm{MeV}/c^2$ ($\approx 2.5\sigma$). A mass-constrained fit is then performed for the signal window candidates, to improve the center-of-mass (CM) momentum $p^*_{J/\psi}$ resolution. QED processes are suppressed by requiring the total charged multiplicity (N_{ch}) in the event to be greater than 4. In the $\Upsilon(4S)$ data J/ψ mesons from $B\bar{B}$ events are removed by requiring $p^*_{J/\psi} > 2.0\ \mathrm{GeV}/c$; no requirement on $p^*_{J/\psi}$ is applied in the continuum data sample. We also reconstruct charmonia decaying to J/ψ. ψ' candidates are reconstructed via the decay to $J/\psi\pi^+\pi^-$, with the ψ' signal window defined by $|M_{J/\psi\pi^+\pi^-} - m_{\psi'}| < 10\ \mathrm{MeV}/c^2$ ($\approx 3\sigma$). χ_{c1} and χ_{c2} candidates are reconstructed using the $J/\psi\gamma$ mode; signal windows of $\pm 20\ \mathrm{MeV}/c^2$ are chosen around the corresponding nominal masses ($\approx 2.5\sigma$). In addition we require $\cos\theta_\gamma < 0$, where θ_γ is defined as the angle between the photon momentum and the CM system, seen from the $\chi_{c1(2)}$ rest frame. This requirement suppresses the large combinatorial background due to low energy photons by more than an order of magnitude, while retaining 50% of the signal, independent of the $\chi_{c1(2)}$ polarization.

Candidate D^0 mesons are reconstructed in the $K^-\pi^+$, K^+K^-, $K^0_S\pi^+\pi^-$, and $K^-\pi^-\pi^+\pi^+$ decay modes [10]. We reconstruct D^+ mesons using $K^-\pi^+\pi^+$, $K^-K^+\pi^+$, $K^0_S\pi^+$, and $K^0_S\pi^+\pi^+\pi^-$ decays; for D_s^+ meson reconstruction we use the $K^-K^+\pi^+$ and $K^0_S\pi^+$; and, finally, Λ_c^+ baryons are reconstructed via $pK^-\pi^+$, pK^0_S, and $\Lambda^0\pi^+$. A $\pm 15\ \mathrm{MeV}/c^2$ mass window ($\approx 2.5\sigma$) is used throughout, except for the $D \to K3\pi^{\pm}$ modes where the resolution is better, and the combinatorial background higher: in these cases, a $\pm 10\ \mathrm{MeV}/c^2$ window is chosen ($\approx 2.3\sigma$). To study the contribution of combinatorial background under the various charmed hadron peaks, we use sidebands selected from a mass window 4 times as large.

We generate large Monte Carlo (MC) samples of double charmonium production, of the process $e^+e^- \to J/\psi c\bar{c}$ with fragmentation to open charm and of $e^+e^- \to J/\psi q\bar{q}$ events. In the MC samples, the J/ψ kinematical characteristics (momentum spectrum and angular distributions) are tuned to those measured in the data. As the measured distributions are extracted from the data using the MC simulation, the tuning procedure is repeated until the difference between successive iterations becomes negligibly small.

To measure the contribution of $c\bar{c}$ resonances to the $e^+e^- \to J/\psi c\bar{c}$ cross section, we reconstruct all double charmonium final states that can result in the presence of a J/ψ in the event: $J/\psi(c\bar{c})_{\mathrm{res}}$, $\psi'(c\bar{c})_{\mathrm{res}}$, and $\chi_{c1(2)}(c\bar{c})_{\mathrm{res}}$, where $(c\bar{c})_{\mathrm{res}}$ is one of the charmonium states below open-charm threshold. If a charmonium state lies above the open-charm threshold [11], we assume it will decay predominantly to charmed hadrons; production of a J/ψ together with charmed hadrons is treated separately below. The process $e^+e^- \to Y(c\bar{c})_{\mathrm{res}}$, where Y is one of the 1^{--} states, recently observed in initial state radiation (ISR) studies [12], can produce J/ψ from Y decays. However, we are unable to measure this contribution because of the large Y intrinsic width, and ignore it. Following the method described in [5,13], we first reconstruct a $(c\bar{c})_{\mathrm{tag}} = J/\psi$, ψ', or $\chi_{c1(2)}$ meson to tag the process, and then form the recoil mass $M_{\mathrm{rec}}((c\bar{c})_{\mathrm{tag}}) = ((E_{\mathrm{CM}} - E^*_{\mathrm{tag}})^2 - p^{*2}_{\mathrm{tag}})^{1/2}$, where E^*_{tag} and p^*_{tag} are the CM energy and momentum of the $(c\bar{c})_{\mathrm{tag}}$, and E_{CM} is the CM energy. The $M_{\mathrm{rec}}((c\bar{c})_{\mathrm{tag}})$ spectra for the data are presented in Fig. 1. We assume that only charmonium states with a charge conjugation eigenvalue opposite to that of $(c\bar{c})_{\mathrm{tag}}$ can appear; two virtual photon annihilation, which can produce a pair of charmonium states with the same eigenvalue, was not observed in Ref. [13], and is expected to be small.

We fit the four $M_{\mathrm{rec}}((c\bar{c})_{\mathrm{tag}})$ spectra simultaneously to fix the $\psi^{(\prime)}\chi_{c1(2)}$ contributions, which are poorly resolved in the $M_{\mathrm{rec}}(\psi^{(\prime)})$ spectra. The ratios of the $\psi^{(\prime)}\chi_{c1(2)}$ signal contributions to the $M_{\mathrm{rec}}(\psi^{(\prime)})$ and $M_{\mathrm{rec}}(\chi_{c1(2)})$ spectra are fixed according to the MC study. The signal line shapes for all the double charmonium final states are obtained from MC simulation, with ISR included, and the background is parameterized by a linear function [a second order polynomial function in the $M_{\mathrm{rec}}(J/\psi)$ case]. Only the region below the open-charm threshold ($M_{\mathrm{rec}} < 3.7\ \mathrm{GeV}/c^2$) is included in the fit. The fitting function for the $M_{\mathrm{rec}}(J/\psi)$ spectrum also includes the expected contribution from the ISR process $e^+e^- \to \psi'\gamma$; its shape and normalization are fixed from the MC simulation. The fit results are shown in Fig. 1 by solid curves; the background function and the $e^+e^- \to \psi'\gamma$ reflection are shown with dashed and dotted curves, respectively. The signal yields and significances for

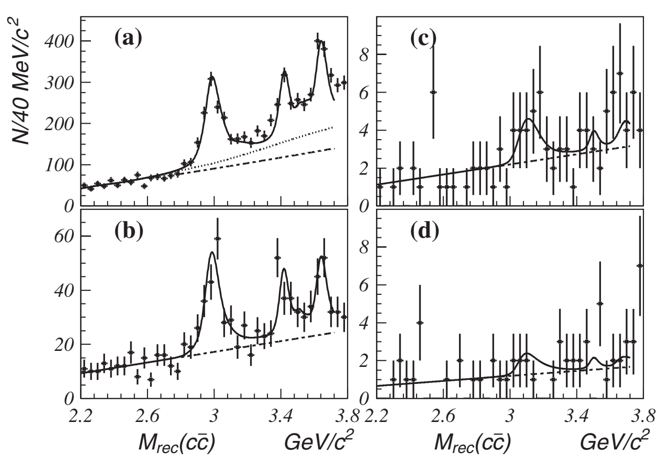

FIG. 1. The $M_{\mathrm{rec}}((c\bar{c})_{\mathrm{tag}})$ spectra: $(c\bar{c})_{\mathrm{tag}} =$ (a) J/ψ, (b) ψ', (c) χ_{c1}, and (d) χ_{c2}. The curves are described in the text.

all the studied double charmonium processes are listed in Table I. The statistical significance of each process is determined from $-2\ln(\mathcal{L}_0/\mathcal{L}_{\max})$, where $\mathcal{L}_{\max}$ is the maximum likelihood returned by the fit, and $\mathcal{L}_0$ is the likelihood with the corresponding contribution set to zero.

Next, we study associated production of a J/ψ with charmed hadrons. In the previous paper [5], we determined the $J/\psi c\bar{c}$ cross section from measurements of the production rate of a J/ψ with associated D^0 and D^{*+} mesons using model predictions for probabilities of fragmentation $c\bar{c} \to D^0(D^{*+})$. Moreover, to suppress combinatorial background from $B\bar{B}$ events, we applied additional kinematical criteria; the efficiency of these criteria also contributed to the model dependence of the result. To eliminate the model dependence in this analysis we use all the ground state charmed hadrons: $H_c = D^0$, D^+, D_s^+, and Λ_c^+, except for $\Xi_c^{0(-)}$ and Ω_c^0 whose production rates in $c\bar{c}$ fragmentation are expected to be smaller than 1% according to the Lund model. As two charmed hadrons are produced in $c\bar{c}$ fragmentation, the $J/\psi c\bar{c}$ cross section is given by half the sum of the $J/\psi H_c X$ cross sections. We extract J/ψ yields in both H_c signal and sideband windows, using fits to $M_{\ell^+\ell^-}$ distributions with signal and second order polynomial background functions. The J/ψ signal shape is obtained from MC simulation, with the small difference in the J/ψ resolution between the MC and data corrected. The $M_{\ell^+\ell^-}$ spectra are shown for D^0, D^+, D_s^+, and Λ_c^+ signal windows in Figs. 2(a)–2(d), respectively; scaled sideband distributions are superimposed. The $J/\psi H_c$ yields are calculated as the difference between the J/ψ yields in the signal window and the (scaled) sidebands. We observe a significant excess J/ψ signal in the D^0 and D^+ signal windows with respect to the corresponding sidebands, demonstrating large $e^+e^- \to J/\psi D^0(D^+)X$ cross sections. The $J/\psi D^0$ and $J/\psi D^+$ yields are 1072 ± 108 and 715 ± 93 events with significances of 10.1σ and 7.8σ, respectively. An excess, with low significance, is also seen in $e^+e^- \to J/\psi D_s^+(\Lambda_c^+)X$: $N_{J/\psi D_s^+} = 129 \pm 42$ (3.2σ) and $N_{J/\psi \Lambda_c^+} = 43 \pm 20$ (2.2σ).

TABLE I. $e^+e^- \to (c\bar{c})_{\rm tag}(c\bar{c})_{\rm res}$ signal yields (significances) from a simultaneous fit to $M_{\rm rec}((c\bar{c})_{\rm tag})$ spectra.

$(c\bar{c})_{\rm res}$	$(c\bar{c})_{\rm tag}$: J/ψ	ψ'	χ_{c1}	χ_{c2}
η_c	$1032 \pm 62(19)$	$161 \pm 22(8.2)$	$\cdots$	$\cdots$
J/ψ	$\cdots$	$\cdots$	$16 \pm 5(3.2)$	$9 \pm 4(2.1)$
χ_{c0}	$525 \pm 54(9.6)$	$75 \pm 19(4.3)$	$\cdots$	$\cdots$
χ_{c1}	$119 \pm 39(3.2)$	12 ± 12	$\cdots$	$\cdots$
h_c	$\cdots$	$\cdots$	4 ± 6	1 ± 5
χ_{c2}	$99 \pm 43(2.1)$	7 ± 16	$\cdots$	$\cdots$
η_c'	$679 \pm 63(10)$	$81 \pm 19(4.5)$	$\cdots$	$\cdots$
ψ'	$\cdots$	$\cdots$	6 ± 6	2 ± 5

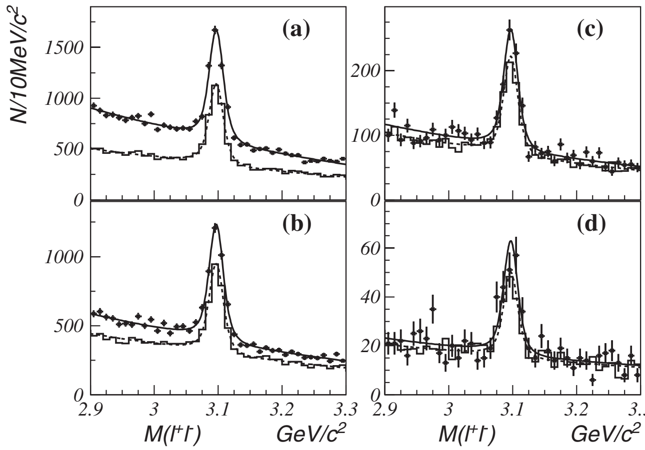

FIG. 2. $M_{\ell^+\ell^-}$ spectra for H_c signal (points with errors) and scaled H_c sideband windows (histograms), where $H_c =$ (a) D^0, (b) D^+, (c) D_s^+, and (d) Λ_c^+. The curves represent the result of the fit; solid curves correspond to the H_c signal windows, and dashed curves to the H_c sidebands.

Next, we measure the J/ψ momentum spectrum in inclusive production and from the process $e^+e^- \to J/\psi c\bar{c}$. The inclusive J/ψ momentum spectrum is obtained by fitting $\ell^+\ell^-$ mass distributions in bins of $p^*_{J/\psi}$ with signal and second order polynomial background functions. In the region $p^*_{J/\psi} < 2.0$ GeV$/c$ only the continuum data is used; the J/ψ yields are then scaled according to the ratio of luminosities. The small contribution from the ISR processes $e^+e^- \to \psi^{(\prime)}\gamma$ ($\sim 2\%$ of the total J/ψ rate) is subtracted using a MC simulation. The final yield in each momentum bin, after subtraction of QED background, is then corrected for the J/ψ reconstruction efficiency and divided by the total luminosity. The resulting differential cross section is shown in Fig. 3(a) with open circles.

We calculate the momentum spectrum of J/ψ mesons from all double charmonium processes, including J/ψ from cascade decays. We use a MC simulation with the contributions of double charmonium processes fixed to the results of the fit to data (Table I) to obtain this spectrum, shown in Fig. 3(a) with filled circles. The momentum spectrum is peaked near the kinematical limit as expected for two-body processes; ISR results in a lower momentum tail, and there is an additional contribution at $p^*_{J/\psi} \sim 3$ GeV$/c$ due to J/ψ's from cascade decays.

To obtain the J/ψ momentum spectrum from the process $e^+e^- \to J/\psi H_c X$, we measure $J/\psi H_c$ yields in bins of $p^*_{J/\psi}$. The fits to $M_{\ell^+\ell^-}$ spectra (Fig. 2) are repeated in the H_c signal and sideband windows for each bin, with the $J/\psi H_c$ yield defined as the fitted J/ψ yield in the H_c mass window after subtraction of the scaled yield in the H_c sidebands. Using the continuum data it is possible to perform such fits below 2 GeV$/c$, though with much larger statistical errors. The yield in each bin is then corrected for the J/ψ and H_c reconstruction efficiencies, using a MC

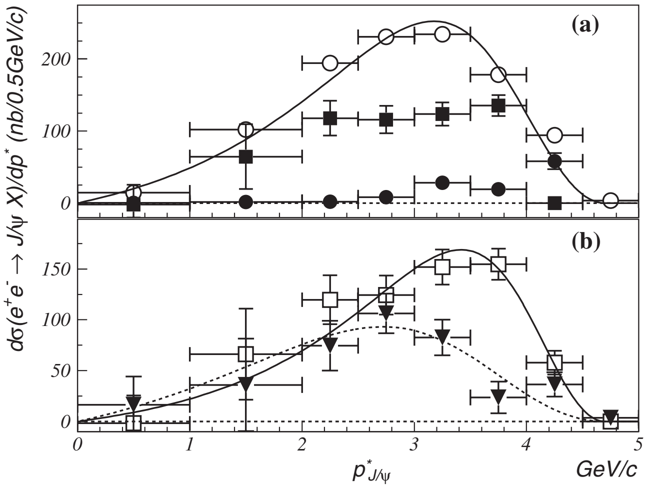

FIG. 3. $p^*_{J/\psi}$ spectra: (a) inclusive (open circles), from $e^+e^- \to J/\psi H_c X$ (filled squares) and from double charmonium production (filled circles); (b) the sum of all $e^+e^- \to J/\psi c\bar{c}$ processes (open squares), from the $e^+e^- \to J/\psi X_{\text{non-}c\bar{c}}$ processes (filled triangles). The fit results are shown in (a) for the inclusive spectrum, and in (b) for the processes $e^+e^- \to J/\psi c\bar{c}$ (solid curve) and $e^+e^- \to J/\psi X_{\text{non-}c\bar{c}}$ (dashed curve).

simulation. The sum over all H_c weighted by a factor of 0.5 is plotted in Fig. 3(a) with filled squares and represents the J/ψ momentum spectrum from the process $e^+e^- \to J/\psi c\bar{c}$, where the $c\bar{c}$ pair fragments into charmed hadrons. The sum of this distribution and that from double charmonium production represents the J/ψ momentum spectrum from the process $e^+e^- \to J/\psi c\bar{c}$; it is shown in Fig. 3(b) by the open squares. The difference between this and the inclusive J/ψ spectrum is thus the spectrum from $e^+e^- \to J/\psi X_{\text{non-}c\bar{c}}$ events, where the system recoiling against the J/ψ is not produced via a $c\bar{c}$ pair (shown by the filled triangles in Fig. 3(b), to which the color-singlet $e^+e^- \to J/\psi gg$ and color-octet $e^+e^- \to J/\psi g$ processes contribute.

The J/ψ momentum spectra, shown in Fig. 3 for the processes $e^+e^- \to J/\psi X$, $J/\psi c\bar{c}$, and $J/\psi X_{\text{non-}c\bar{c}}$, are then used to calculate the respective cross sections, after summing over all momentum bins. The results are presented in Table II. The statistical errors are dominated by the momentum interval $p^*_{J/\psi} < 2.0$ GeV/c, where only the

TABLE II. Cross sections for the processes $e^+e^- \to J/\psi X$, $J/\psi c\bar{c}$, and $J/\psi X_{\text{non-}c\bar{c}}$ ([pb]), and characteristics of the J/ψ spectra (ϵ_{Pet}, α_{hel}, and α_{prod}); χ^2/n_{dof} values for the corresponding fits are listed in parentheses.

	$J/\psi X$	$J/\psi c\bar{c}$	$J/\psi X_{\text{non-}c\bar{c}}$
σ	1.17 ± 0.02	0.74 ± 0.08	0.43 ± 0.09
σ_{Pet}	1.19 ± 0.01	0.73 ± 0.05	0.48 ± 0.07
ϵ_{Pet}	$0.16 \pm 0.01(8.9)$	$0.10 \pm 0.02(0.6)$	$0.32^{+0.16}_{-0.12}(1.6)$
α_{hel}	$0.03 \pm 0.03(0.6)$	$-0.19^{+0.25}_{-0.22}(1.0)$	$0.41^{+0.60}_{-0.45}(1.2)$
α_{prod}	$0.69 \pm 0.05(3.3)$	$-0.26^{+0.24}_{-0.22}(0.5)$	$5.2^{+6.1}_{-2.4}(0.3)$

small continuum data sample is used. The contribution to the $J/\psi c\bar{c}$ cross section from all double charmonium final states is (0.12 ± 0.02) pb. The calculated cross sections for individual $J/\psi H_c X$ are (0.63 ± 0.11) pb ($H_c = D^0$), (0.45 ± 0.09) pb ($H_c = D^+$), (0.10 ± 0.07) pb ($H_c = D_s^+$), and (0.06 ± 0.05) pb ($H_c = \Lambda_c^+$). To characterize the hardness of the momentum spectrum, we perform fits using the Peterson function [14]; the parameters ϵ_{Pet} for the $e^+e^- \to J/\psi c\bar{c}$ and $J/\psi X_{\text{non-}c\bar{c}}$ processes are listed in Table II. For completeness, the resulting cross sections σ_{Pet} are also shown: they are consistent with the directly calculated values, with statistical errors reduced. Such results are model dependent, and we rely instead on the directly calculated values σ for the cross section.

We note that unlike our first paper [15] no correction for the N_{ch} requirement is applied for any of the process studied. For $e^+e^- \to J/\psi X_{\text{non-}c\bar{c}}$ such corrections are only possible by relying on a model. However, for the process $e^+e^- \to J/\psi c\bar{c}$, the efficiency of the $N_{\text{ch}} > 4$ requirement is more than 99% if the $c\bar{c}$ pair fragments into charmed hadrons. For double charmonium production the efficiency is 70% according to the model used in the MC generator, and varies by $\pm 20\%$ with different charmonium decay models. As double charmonium represents only $\sim 10\%$ of the total $e^+e^- \to J/\psi c\bar{c}$ cross section, the resulting correction is small, and included in the systematic error.

We also perform an angular analysis for the $e^+e^- \to J/\psi c\bar{c}$ and $e^+e^- \to J/\psi X_{\text{non-}c\bar{c}}$ processes. This provides important information on the production mechanisms, and allows the efficiency calculation to be improved: the J/ψ reconstruction efficiency depends on both the production angle (θ_{prod}, the angle between the J/ψ momentum and the beam axis in the CM frame) and the helicity angle (θ_{hel}, the angle between the ℓ^+ from J/ψ decay and the CM, seen from the J/ψ rest frame). The MC simulation is adjusted to match the measured distributions. Angular distributions are obtained from fitted yields in bins of $|\cos\theta_{\text{prod}}|$ and $|\cos\theta_{\text{hel}}|$, with an appropriate efficiency correction performed bin-by-bin, for inclusive J/ψ, J/ψ from double charmonium production, and J/ψ from $e^+e^- \to J/\psi H_c X$. The results are shown in Fig. 4. The inclusive J/ψ distributions (open circles) are obtained from J/ψ yields. Those for double charmonium production are obtained from fits to the four $M_{\text{rec}}((c\bar{c})_{\text{tag}})$ distributions, as for Fig. 1 above. Distributions for $e^+e^- \to J/\psi H_c X$ are obtained from fitted J/ψ yields in appropriate H_c mass windows, after subtraction of yields in the H_c sidebands. The distributions for $e^+e^- \to J/\psi c\bar{c}$ (open squares) are calculated as the sum of the corresponding distribution for double charmonium production (with weight 1.0) and $e^+e^- \to J/\psi H_c X$ (with weight 0.5). Distributions for the $e^+e^- \to J/\psi X_{\text{non-}c\bar{c}}$ process (filled triangles) are determined from the difference between $e^+e^- \to J/\psi X$ inclusive and $J/\psi c\bar{c}$ distributions in each bin.

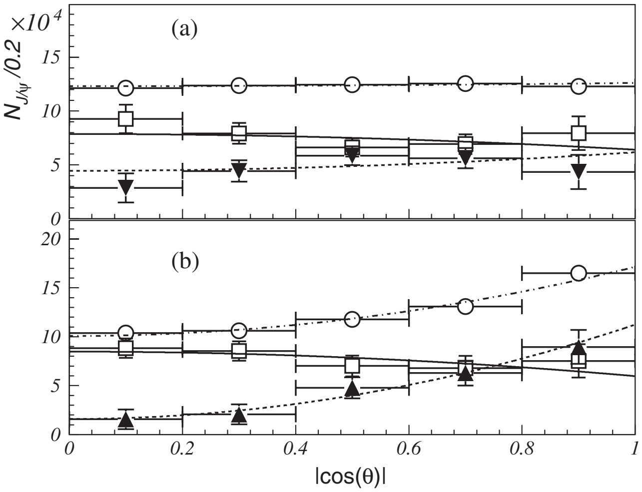

FIG. 4. Angular distributions [$|\cos\theta_{\rm hel}|$ in (a), $|\cos\theta_{\rm prod}|$ in (b)] for inclusive $e^+e^- \to J/\psi X$ (open circles), $e^+e^- \to J/\psi c\bar{c}$ (open squares), and $e^+e^- \to J/\psi X_{\text{non-}c\bar{c}}$ processes (filled triangles). The results of the fits described in the text are shown with the dash-dotted, solid, and dashed curves, respectively.

We fit the helicity angle distribution with a function $\sim(1+\alpha_{\rm hel}\cos^2(\theta_{\rm hel}))$. While the production angle distributions are also fitted with a function $\sim(1+\alpha_{\rm prod}\cos^2(\theta_{\rm prod}))$, we note that these distributions can differ from $1+\alpha\cos^2\theta$ due to ISR or the contribution of the $e^+e^- \to \gamma^*\gamma^* \to J/\psi X$ process to the $J/\psi X_{\text{non-}c\bar{c}}$ final state. The fits yield the parameters $\alpha_{\rm hel}$ and $\alpha_{\rm prod}$ listed in Table II; the fit results are shown in Fig. 4.

The systematic errors on the production cross sections for both $e^+e^- \to J/\psi c\bar{c}$ and $J/\psi X_{\text{non-}c\bar{c}}$ processes are summarized in Table III. In the double charmonium production study, systematic errors due to J/ψ yield fitting are determined as in our previous papers [5,13]; we also perform variant fits including final states with two charmonia with the same charge conjugation eigenvalue. In the study of associated production, we consider changes in $J/\psi H_c$ yields under variation of the fitting procedure [a two-dimensional fit to $(M(J/\psi), M(H_c))$, a fit to the $M(J/\psi)$ distribution in bins of $M(H_c)$, and to the $M(H_c)$ in bins of $M(J/\psi)$], as well as variation of the signal and background parameterizations, the fit ranges, and the binning. The uncertainty in H_c reconstruction efficiencies due to the unknown kinematics of $c\bar{c}$ fragmentation into charmed hadrons is small, due to the weak dependence of reconstruction efficiency on H_c momentum, and is included in the total systematic error.

TABLE III. Summary of the systematic errors on the cross sections shown, in percent.

Source	$J/\psi X$	$J/\psi c\bar{c}$	$J/\psi X_{\text{non-}c\bar{c}}$
Fitting procedure	±3	±5	±9
Angular distributions	±4	±6	±10
$N_{\rm ch}$ requirement	...	$^{+5}_{-0}$	...
ISR	...	$^{+4}_{-2}$	$^{+4}_{-7}$
Track reconstruction	±2	±5	±8
Identification	±2	±4	±7
$\mathcal{B}(J/\psi)$, $\mathcal{B}(H_c)$	±1	±3	±3
Total	±6	$^{+12}_{-11}$	±20

When the integral J/ψ production and helicity angle distributions in the MC simulation are tuned to those in the data, their correlations are not taken into account. We assume the most conservative correlations, resulting in the largest deviation of the J/ψ reconstruction efficiencies that reproduce the integral distributions. The resulting difference in efficiency is the largest contribution to the systematic error. Other contributions come from the uncertainty in the track and $K_S^0(\Lambda^0)$ reconstruction efficiencies; from lepton, kaon and proton identification; and from uncertainties in absolute H_c branching fractions.

In summary, we have measured the cross sections for the processes $e^+e^- \to J/\psi X$, $J/\psi c\bar{c}$, and $J/\psi X_{\text{non-}c\bar{c}}$ to be $(1.17 \pm 0.02 \pm 0.07)$ pb, $(0.74 \pm 0.08\,^{+0.09}_{-0.08})$ pb, and $(0.43 \pm 0.09 \pm 0.09)$ pb, respectively. We therefore conclude that $e^+e^- \to J/\psi c\bar{c}$ is the dominant mechanism for J/ψ production in e^+e^- annihilation, contrary to earlier NRQCD predictions. Moreover, this cross section exceeds the perturbative QCD prediction $\sigma(e^+e^- \to c\bar{c}c\bar{c}) \approx 0.3$ pb [16], which includes the case of fragmentation into four charmed hadrons, rather than $J/\psi c\bar{c}$. The $e^+e^- \to J/\psi c\bar{c}$ process is dominated by $c\bar{c}$ fragmentation to open charm, with only a $(16 \pm 3)\%$ contribution from double charmonium production. The cross section for $J/\psi X_{\text{non-}c\bar{c}}$, which can proceed via $e^+e^- \to J/\psi g(g)$ or $e^+e^- \to J/\psi\gamma^*$ diagrams, is of the same order as that for $J/\psi c\bar{c}$. Recently, $\sigma(e^+e^- \to J/\psi gg)$ has been recalculated including NLO corrections to be ≈ 0.5 pb, consistent with our measurement [17].

We have measured the J/ψ momentum spectrum and the production and helicity angle distributions from all three processes. For the $e^+e^- \to J/\psi X_{\text{non-}c\bar{c}}$ process, the J/ψ momentum spectrum is significantly softer than that for $e^+e^- \to J/\psi c\bar{c}$, and the production angle distribution peaks along the beam axis. We note that all the measured cross sections are full (rather than Born) cross sections and include contributions from cascade J/ψ, and that model-dependent corrections for the charged track multiplicity requirement have not been performed.

We thank the KEKB group for excellent operation of the accelerator, the KEK cryogenics group for efficient solenoid operations, and the KEK computer group and the NII for valuable computing and Super-SINET network support. We acknowledge support from MEXT and JSPS (Japan); ARC and DEST (Australia); NSFC and KIP of CAS (China); DST (India); MOEHRD, KOSEF, and KRF (Korea); KBN (Poland); MES and RFAAE (Russia); ARRS (Slovenia); SNSF (Switzerland); NSC and MOE (Taiwan); and DOE (USA).

[1] P. Cho and A. K. Leibovich, Phys. Rev. D **53**, 150 (1996); **53**, 6203 (1996); S. Baek, P. Ko, J. Lee, and H. S. Song, J. Korean Phys. Soc. **33**, 97 (1998).
[2] F. Yuan, C.-F. Qiao, and K.-T. Chao, Phys. Rev. D **56**, 321 (1997).
[3] V. V. Kiselev, A. K. Likhoded, and M. V. Shevlyagin, Phys. Lett. B **332**, 411 (1994).
[4] A. V. Berezhnoy and A. K. Likhoded, Yad. Fiz. **67**, 778 (2004); [Phys. At. Nucl. **67**, 757 (2004)].
[5] K. Abe *et al.* (Belle Collaboration), Phys. Rev. Lett. **89**, 142001 (2002).
[6] Y.-J. Zhang and K.-T. Chao, Phys. Rev. Lett. **98**, 092003 (2007).
[7] A. B. Kaidalov, JETP Lett. **77**, 349 (2003).
[8] A. Abashian *et al.* (Belle Collaboration), Nucl. Instrum. Methods Phys. Res., Sect. A **479**, 117 (2002); Z. Natkaniec *et al.* (Belle Collaboration), Nucl. Instrum. Methods Phys. Res., Sect. A **560**, 1 (2006).
[9] S. Kurokawa and E. Kikutani, Nucl. Instrum. Methods Phys. Res., Sect. A **499**, 1 (2003), and other papers included in this volume.
[10] Charge-conjugate modes are included throughout this paper.
[11] K. Abe *et al.* (Belle Collaboration), Phys. Rev. Lett. **98**, 082001 (2007).
[12] B. Aubert *et al.* (*BaBar* Collaboration), Phys. Rev. Lett. **95**, 142001 (2005).
[13] K. Abe *et al.* (Belle Collaboration), Phys. Rev. D **70**, 071102 (2004).
[14] C. Peterson, D. Schlatter, I. Schmitt, and P. M. Zerwas, Phys. Rev. D **27**, 105 (1983).
[15] K. Abe *et al.* (Belle Collaboration), Phys. Rev. Lett. **88**, 052001 (2002).
[16] A. V. Berezhnoy and A. K. Likhoded, Phys. At. Nucl. **70**, 478 (2007).
[17] Y.-Q. Ma, Y.-J. Zhang, and K.-T. Chao, arXiv:0812.5106.